Supplement of Hydrol. Earth Syst. Sci., 27, 4563–4577, 2023
https://doi.org/10.5194/hess-27-4563-2023-supplement

Hydrology and Earth System Sciences
Open Access
EGU

Supplement of

The most extreme rainfall erosivity event ever recorded in China up to 2022: the 7.20 storm in Henan Province

Yuanyuan Xiao et al.

Correspondence to: Shuiqing Yin (yinshuiqing@bnu.edu.cn)

Supplement

S1: Estimation of rainfall erosivity from the different kinetic energy–intensity (KE-I) equations

Table S1.1: Different versions of KE-I equations.

Version	KE-I equation
USLE (Wischmeier and Smith, 1978)	$e_r = \begin{cases} 0.119 + 0.0873 \cdot log_{10}(i_r) & i_r \leq 76\, mm \cdot h^{-1} \\ 0.283 & i_r > 76\, mm \cdot h^{-1} \end{cases}$
RUSLE (Renard et al., 1997)	$e_r = 0.29 \cdot [1 - 0.72 \cdot exp(-0.05 \cdot i_r)]$
RUSLE 2 (USDA–ARS, 2013)	$e_r = 0.29 \cdot [1 - 0.72 \cdot exp(-0.082 \cdot i_r)]$
Dijk (van Dijk et al., 2002)	$e_r = 28.3 \cdot [1 - 0.52 \cdot exp(-0.042 \cdot i_r)]$

Table S1.2: Comparison of the maximum event kinetic energy (KE) and return period (RP) from the KE-I equations of USLE, RUSLE and van Dijk's with those from the RUSLE2. DE: relative difference.

	The "7.20" storm		Event kinetic energy (1951-2020)		RP (years)
	KE (MJ·ha^{-1})	DE	KE (MJ·ha^{-1})	DE	
RUSLE2	195.8	0	5.1 ~ 49.7	0	19,200
USLE	190.2	-3.1%	5.4 ~ 46.7	-8.7% ~ 23.1%	39,100
RUSLE	179.6	-8.2%	4.5 ~ 46.6	-16.9% ~ -2.0%	23,900
van Dijk	184.0	-6.1%	5.0 ~ 46.2	-11.8% ~ 28.7%	51,800

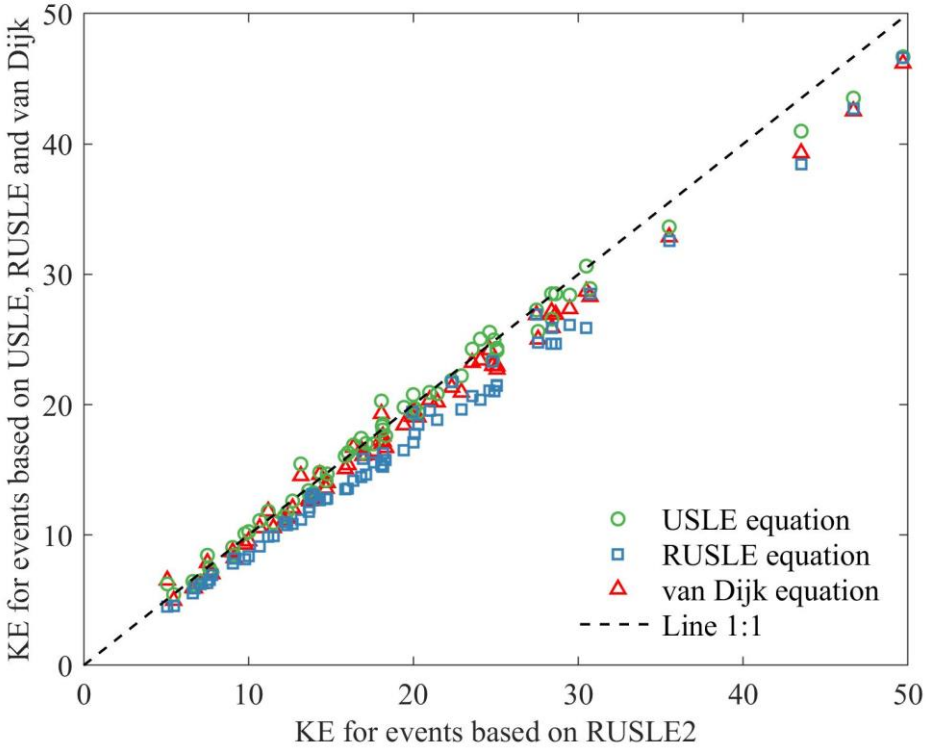

Figure S1.1: Comparison of the annual maximum event kinetic energy (KE) using four different KE-I equations for Zhengzhou meteorological station from 1951-2020.

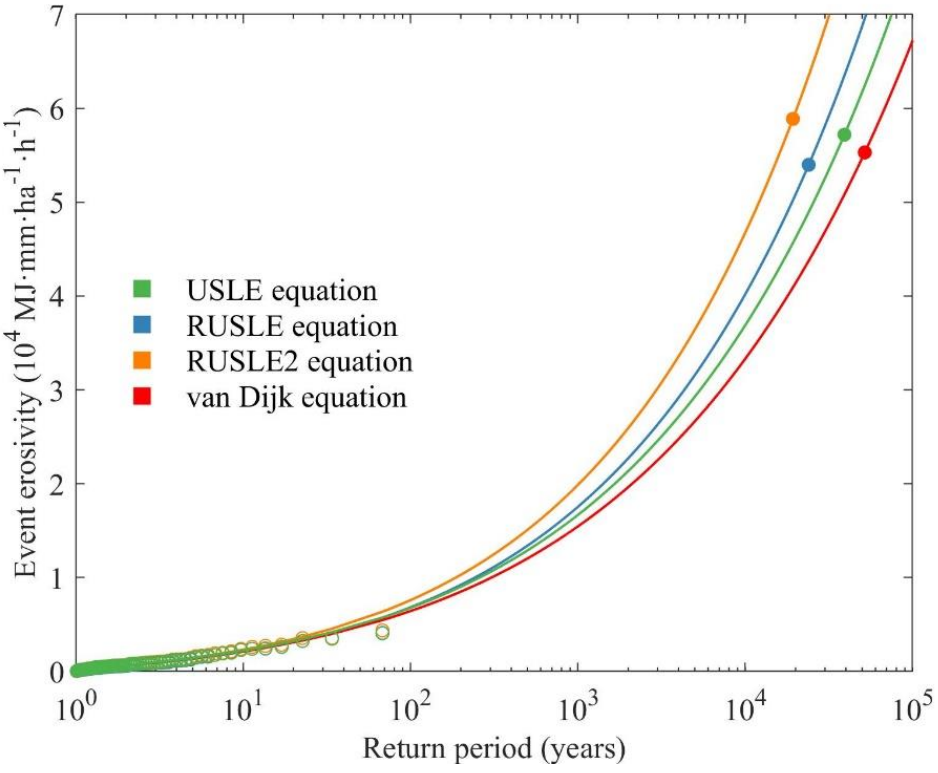

Figure S1.2: Observed event rainfall erosivity as a function of the return period assuming LP-III using four different KE-I equations for Zhengzhou meteorological station. The open circles are observations for the period 1951-2020, the solid circles indicate the "7.20" storm in 2021, and the solid lines represent the fitted P-III distribution using the logarithm of observations from 1951-2020.

S2: Calculation of conversion factor

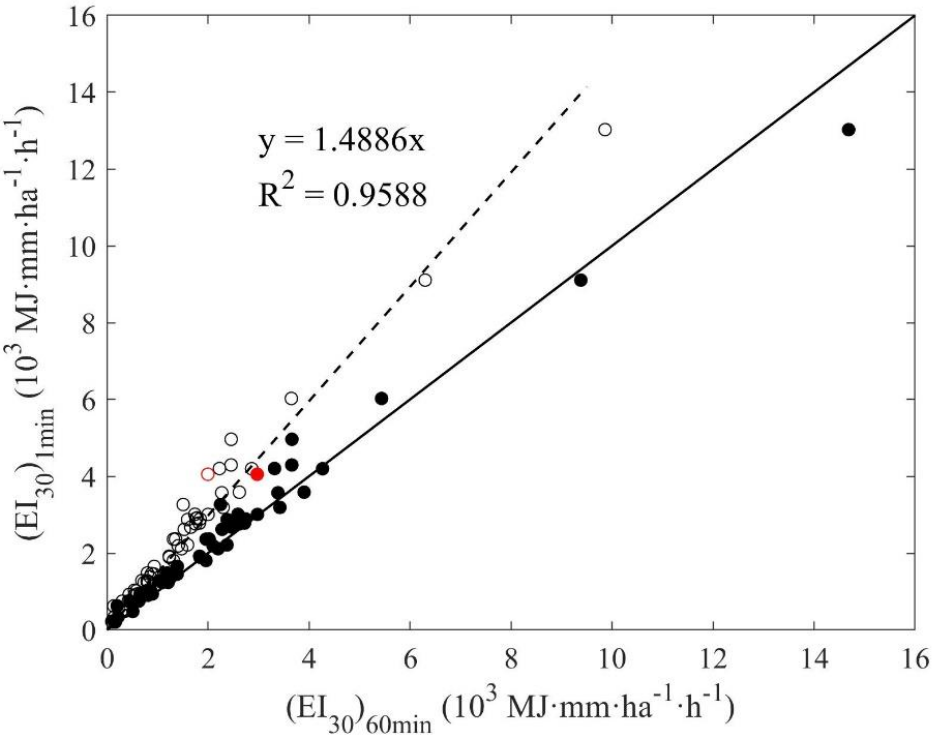

Figure S2.1: A comparison of 1-in-10-year EI_{30} values estimated with one-min versus 60-min data. The dashed line represents the best fit using a linear model through the origin. Open circles are 1-in-10-year EI_{30} values estimated 60-min data without conversions, and solid circles are values adjusted with a conversion factor of 1.489 for the 62 meteorological stations in China. The open and solid circles in red refer to the Zhengzhou meteorological station. (Yue et al., 2020)

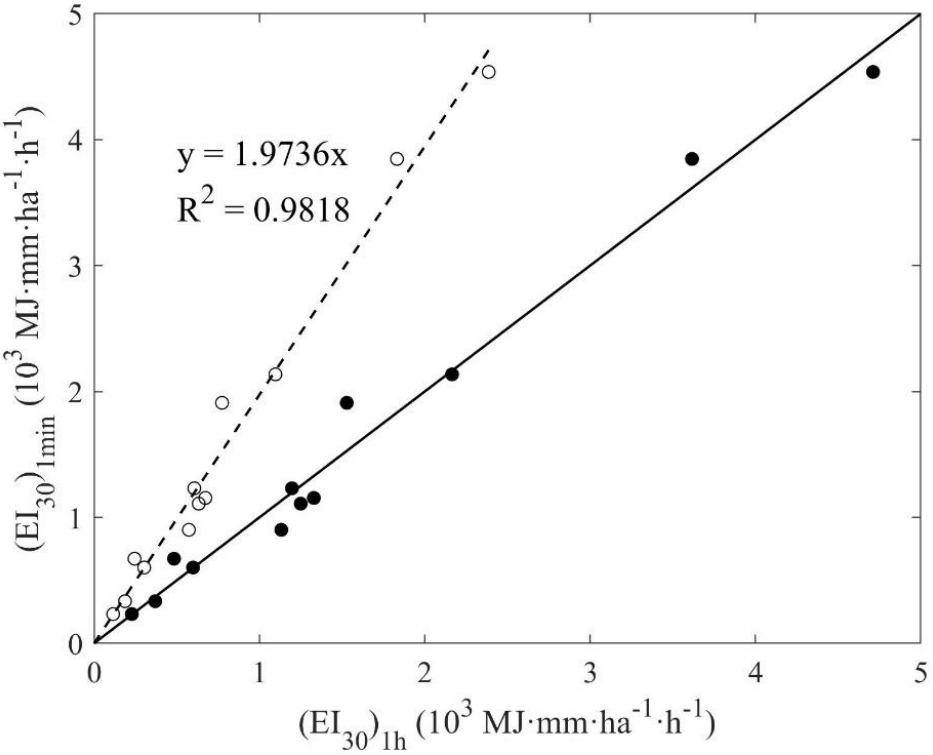

Figure S2.2: A comparison of annual maximum EI_{30} values estimated with one-min versus one-hour data in Zhengzhou meteorological station from 2005 to 2016. The dashed line represents the best fit using a linear model through the origin. Open circles are EI_{30} values estimated one-hour data without conversions, and solid circles are values adjusted with a conversion factor of 1.974 for the Zhengzhou meteorological station.

S3: Testing of three frequency distributions

Table S3.1: Generalized extreme value (GEV) and P-III distribution used in hydrology. Method of L-moments was used for the parameter estimation of GEV (Hosking, 1990). (PDF: probability density function; CDF: cumulative distribution function; Γ(α): gamma function)

Distribution	GEV	Reference
PDF	$f(x) = \frac{1}{\sigma}[1 - k(\frac{x-\mu}{\sigma})]^{1/k-1} e^{-[1-k(\frac{x-\mu}{\sigma})]^{1/k}}$	Coles,1990; Jenkinson, 1955
CDF	$F(x) = e^{-[1-k(\frac{x-\mu}{\sigma})]^{1/k}}$	
Range	$k \neq 0$	
Distribution	**P-III**	**Reference**
PDF	$f(x) = \frac{\beta^{\alpha}}{\Gamma(\alpha)}(x - a_0)^{\alpha-1} e^{-\beta(x-a_0)}$	Ministry of Water Resources, P. R. C., 2006
CDF	$F(x) = \frac{\beta^{\alpha}}{\Gamma(\alpha)} \int_{a_0}^{x} (x - a_0)^{\alpha-1} e^{-\beta(x-a_0)} dx$	
Range	$x > a_0, \alpha > 0, \beta > 0$	

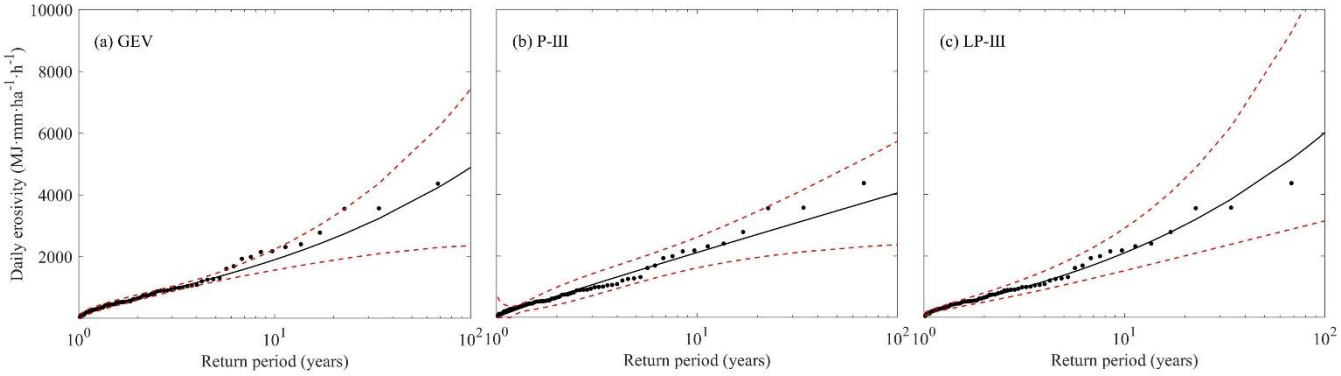

Figure S3.1: Observed daily rainfall erosivity as a function of the return period assuming (a) GEV, (b) P-III and (c) LP-III for Zhengzhou meteorological station. Black solid circles are observations from the period 1951-2020. The dashed lines represent the 95% confidence interval.

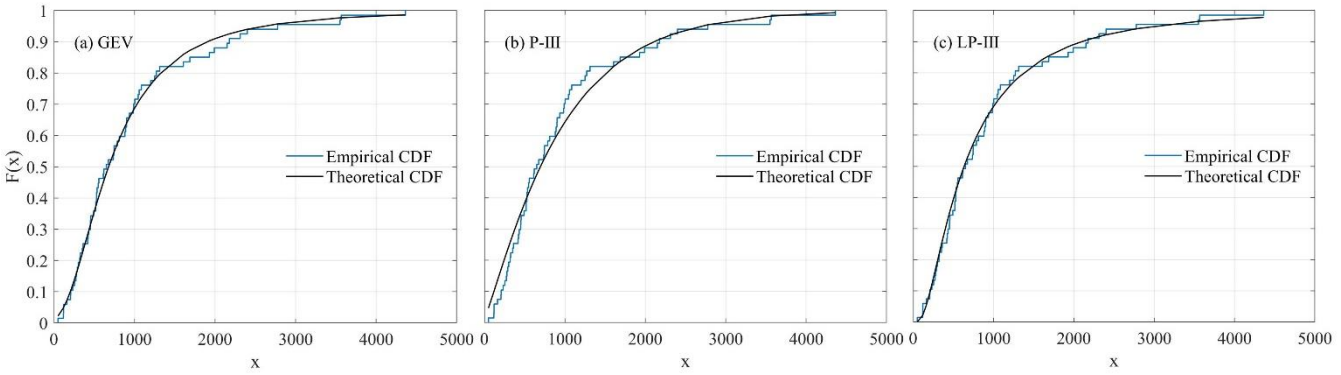

Figure S3.2: The cumulative distribution function of (a) GEV, (b) P-III and (c) LP-III of observed daily rainfall erosivity for Zhengzhou meteorological station.

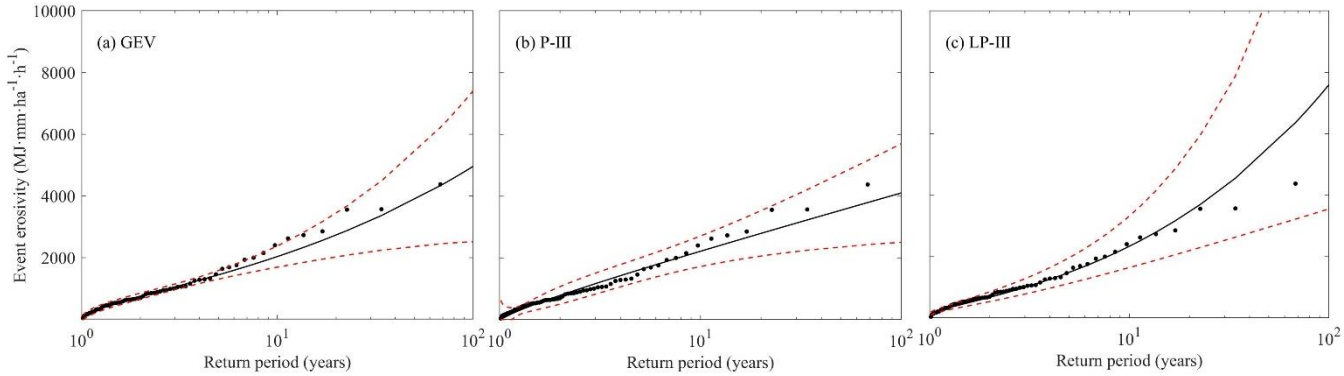

Figure S3.3: Observed event rainfall erosivity as a function of the return period assuming (a) GEV, (b) P-III and (c) LP-III for Zhengzhou meteorological station. Black solid circles are observations from the period 1951-2020. The dashed lines represent the 95% confidence interval.

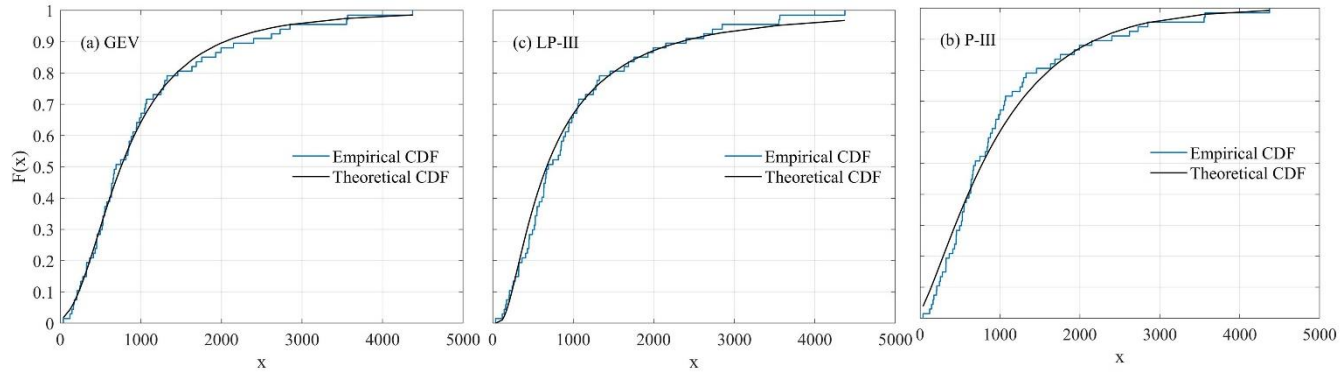

Figure S3.4: The cumulative distribution function of (a) GEV, (b) P-III and (c) LP-III of observed event rainfall erosivity for Zhengzhou meteorological station.

Table S3.2. Correlation coefficient (CC) Kolmogorov-Smirnov test (K-S test) of daily and event rainfall erosivity.

	Statistical Metrics	GEV	P-III	LP-III
Daily erosivity	CC	0.9820	0.9849	0.9907
	K-S value	0.0574	0.0950	0.0642
	p-value	0.9708	0.5483	0.9286
	Return periods	65,500	+∞	53,700
Event erosivity	CC	0.9791	0.9868	0.9790
	K-S value	0.0507	0.0849	0.0853
	p-value	0.9919	0.6870	0.6818
	Return periods	340,600	+∞	19,200

Statistics used in Table S3.2:

In order to assess the goodness-of-fit (GOF) of the GEV, P-III, and LP-III Gumbel distributions, using the Kolmogorov-Smirnov (K-S) test (Haktanir, 1991). The smaller the value of the K-S test statistic, the better the fitting of the distribution. Correlation coefficient (CC) was chosen to measure the difference between the estimated value and the measured data (see Eq. (1)). CC was used to represent the level of agreement between P datasets and gauge observations.

$$CC = \frac{\sum_{i=1}^{n}(S_i-\bar{S})\cdot(G_i-\bar{G})}{\sqrt{\sum_{i=1}^{n}(S_i-\bar{S})^2\cdot\sum_{i=1}^{n}(G_i-\bar{G})^2}} \quad (1)$$

where n is the number of years or the sample size; i is the i^{th} of the estimated value and the measured data; G_i means observations and $\overline{G}$ is the average of observation. S_i and $\overline{S}$ are the estimated values and their average, respectively.

Reference

Coles, S.: An introduction to statistical modeling of extreme values, New York, Springer Verlag, 36–78, 1990.

Haktanir, T.: Practical computation of gamma frequency factors, Hydrol. Sci. J., 36(6): 599-610, 1991.

Hosking, J. R. M.: L-Moments: Analysis and Estimation of Distributions Using Linear Combinations of Order Statistics, J. R. Stat, Soc., Ser. B., Methodol., 52, 105–124, http://www.jstor.org/stable/2345653, 1990.

Jenkinson, A. E.: The frequency distribution of the annual maximum (or minimum) values of meteorological elements, Q. J. R. Meteorol. Soc., 81(348): 158-171, 1955.

Ministry of Water Resources, P. R. C.: Some suggestions of strengthening flood control construction in Taihu Basin, 2001-2010, Beijing: China Water Power Press, 2001 (in Chinese).

Renard, K. G., Foster, G. R., Weesies, G. A., McCool, D. K., and Yoder, D. C.: Predicting soil erosion by water: a guide to conservation planning with the revised universal soil loss equation (RUSLE), Agriculture Handbook, US Department of Agriculture, Washington, D. C., 1997.

USDA-ARS.: Science documentation: Revised universal soil loss equation version2 (RUSLE2), US Department of Agriculture, Agricultural Research Service, Washington, D.C., 2013.

van Dijk, A. I. J. M., Bruijnzeel, L. A., and Rosewell, C. J.: Rainfall intensity–kinetic energy relationships: A critical literature appraisal, J. Hydrol., 261: 1–23, https://doi.org/10.1016/S0022-1694(02)00020-3, 2002.

Wischmeier, W. H. and Smith, D. D.: Predicting rainfall erosion losses: A guide to conservation planning, Agriculture Handbook, US Department of Agriculture, Washington, D. C., 1978.

Yue, T. Y., Xie, Y., Yin, S. Q., Yu, B. F., Miao, C. Y., and Wang, W. T.: Effect of time resolution of rainfall measurements on the erosivity factor in the USLE in China, ISWCR, 8, 373–382, https://doi.org/10.1016/j.iswcr.2020.06.001, 2020.